Chapter 1

Introduction

1.1 General introduction

The transition metal oxides are a class of materials with a wide range of electronic properties. The origin of this versatile behavior is rooted in the chemical bonding of the d-electrons, which is between strong covalent bonding, typical of the p-block elements, and metallic bonding of the s-block elements. This intermediate strength chemical bonding results in variable spin, charge and orbital states, which combined with an enormous variety of crystal structures, yields a rich field for fundamental research and technological applications.

There are many properties that have been studied in recent years. The high-T_c superconductors made from copper-oxides challenge our understanding of collective electronic behavior, and has resulted in a resurgence to understand low-dimensional spin- and charge transport. The colossal magnetoresistance materials have resulted in renewed interest how the electronic degrees of freedom interact with the lattice. This class of materials, mostly based on manganese oxides, displays a wealth of interrelated ordering phenomena of magnetic, charge and orbital origin. The valence changes of the transition metal oxides form the basis for ionic conductivity, which is the basis for modern batteries and oxygen diffusion. The piezo- and ferro-electric oxides are often based on early transition metal oxides, in which the formally empty d-shell results in off-centered ions, and thus non-centrosymmetric structures. This finds applications in sensors, actuators an transducers, but also in non-linear optical activity.

In this thesis we focus on two different subsets of materials, the vanadates, and the perovskites (cobaltates and manganites). The vanadates form an interesting class of materials due to the various kinds of oxygen coordination (octahedral, tetrahedral, trigonal, square pyramidal, etc.) with not only three-dimensional but also lower dimensional electronic behavior. Furthermore, vanadium can adopt several valence states from V^{2+} to V^{5+},

including mixed valence states. The d^1 valence state has been recognized as being complementary to the d^9 valence states of the cuprates. For this reason S = 1/2 square lattices have received considerable attention. A modification of the square lattices are the ladder systems, which are theoretically attractive as a basis for the square planar systems. A diverse number of ladder systems has been synthesized in recent years including single, double and triple leg ladders, and also other patterns.

The V_2O_5 based systems have several similarities with the cuprates. These vanadates can be considered as planar systems in which the transition metal has a square pyramidal oxygen coordination, very similar to the copper coordination in several high-T_c superconductors. The chemical bonding can result in a metal-insulator transition, and VO_2 and moreover V_2O_3 are considered to be textbook examples of Mott transitions. The Magnéli phases V_nO_{2n-1} form the structural basis for different geometries. This basis can be modified and several elements can be inserted in the interstitial sites of the layers. This way a large variety of low-dimensional spin systems has been created with *e.g.* CaV_2O_5 a system with a spin gap, and CaV_3O_7 and CaV_4O_9 exhibiting remarkable magnetic properties [1]. The AV_2O_5 compounds with magnetic V^{4+} ions (d^1, S = 1/2) have been intensively studied due to the various kinds of quantum spin phenomena, such as spin-Peierls transition and spin gap [2]. These compounds with layered structures form low-dimensional magnetic systems, such as one-dimensional chain, zigzag chain, ladder, and dimer. In the first part of this thesis we focus on the magnetic singlet formation in the mixed-valent compound NaV_2O_5.

The second part of the thesis is dedicated to the orbital ordering investigation in $LaCoO_3$ and $RMnO_3$ perovskites. These compounds are part of the class of transition metal oxides with the general formula $RTMO_3$ (where R is a rare-earth ion and TM is a transition metal ion). The relatively simple structure of the perovskites consisting of corner shared octahedra can result in versatile ordering patterns. These compounds undergo order-disorder transitions with changes in charge, spin, orbital and lattice degrees of freedom. The most studied compounds with a perovskite structure are the manganese oxides due to their magnetoresistive and magneto-ferro-electric properties. Under specific conditions, *i.e.* temperature, magnetic field and pressure, or by chemical doping with holes, a large variety of phases are obtained, with ordering patterns of spins, charge and/or orbitals. In mixed-valent manganites, the valence electrons can be either localized or free to move between the neighboring manganese sites depending on the relative strengths of two competing processes: the double exchange and the Jahn-Teller effect. The double exchange mechanism involve a two-step process in which the electrons jump between neighboring Mn^{3+} and Mn^{4+} ions being mediated by the ligand oxygens. The double exchange interaction aligns

the spins of the itinerant e_g valence electrons with the localized t_{2g} spins, resulting in a ferromagnetic metallic state. The competing Jahn-Teller effect distorts locally the oxygen octahedron surrounding each manganese atom and tends to localize the valence electrons. At low temperatures and low doping concentrations where the double exchange is not dominant, the electrons are localized with the spins antiferromagnetically coupled due to the superexchange process. For larger doping concentration, the double exchange can stabilize at low temperatures a spin ordered phase (ferromagnetic state), while the dominant effect of the electron-phonon interaction stabilizes a charged ordered phase.

The double exchange mechanism in conjunction with the effects of lattice distortion is believed to be responsible for the occurrence in manganites of the large decrease of resistance induced by application of a magnetic field (CMR effect). Aside from these two competing processes, there is also a large spin splitting of the conduction band with the conduction electrons nearly perfectly spin polarized (half metallic state). While it is commonly accepted that spin and charge state determine the electronic properties in transition metal oxides, it has become of recent interest to study the consequences of the orbital degeneracy on physical properties. For insulating materials long-range ordering of degenerate d-orbitals accompanied by cooperative Jahn-Teller distortion effect is expected to take place below a transition temperature. This orbital ordering can have pronounced effects on physical properties such as metal-insulator transition and charge ordering. The metal-insulator transitions accompanied by dramatic changes in the electronic properties make the transition metal oxides a class of materials with potential for future technological applications. The control of the electronic and magnetic phases using a wide range of tuning parameters may provide a basis for novel electronics.

The techniques we use for our study are powder and single crystal x-ray diffraction. For the transition metal oxides, the structural transitions are often difficult to analyze. The distortions from the high-symmetry parent phase are often small and some of the symmetry elements can be mimicked by twinning. Therefore, the identification of the symmetry is highly nontrivial, and often different measurements techniques are interpreted with a different symmetry. Even diffraction studies may result in competing models of different symmetry. Nevertheless, a correct assignment of the crystal lattice symmetry is quintessential for the interpretation of physical phenomena in oxides.

1.2 Diffraction techniques: SXD versus PXD

Single crystal x-ray diffraction (SXD) is a very versatile method to determine the crystal structure of a wide range of materials. The method is based on measurement of the intensity of Bragg reflections. The integrated intensity of a Bragg reflection I(h k l) is related to the Fourier component of the electron density distribution of the single crystal. Thus, the symmetry of the crystal is reflected in the symmetry of the intensity distribution of the reciprocal lattice. By measurements of the intensities of the reciprocal lattice, the symmetry elements of the structure can be determined. However, the conventionally used diverging x-ray beam geometry does not allow precise determination of the peak position of the reciprocal lattice points. In powder x-ray diffraction (PXD), symmetry related reflections superimpose to single peaks in the diffractogram, and therefore this information about the symmetry is lost. However, the high angular resolution of the PXD technique due to the focusing geometry, allows a very accurate determination of the peak positions. Reflections becoming inequivalent at phase transitions due to loss of particular symmetry will appear at (slightly) different diffraction angles (2θ), resulting in splitting or asymmetric shape of the peaks in the powder diffractogram. Therefore a careful analysis of the peak positions and profiles allows detection of lowering of the symmetry. As the lattice parameters are determined from the peak positions only, they can be accurately refined if the correct space group model is used.

Thus the two methods, SXD and PXD give complementary information. The interpretation of a large part of the results presented in this thesis is based on space group determination, therefore we will focus in this chapter on the SXD technique. After the description of the diffactometers and the types of scans used for the SXD measurements, we will present the main aspects concerning the space group determination. In particular, we will discuss twinning as a main obstacle in symmetry analysis. The last part is dedicated to the description of the bond valence sum method and of the resonance x-ray scattering technique. These methods are used in the Chapter 2 for the SXD analysis of the charge ordering pattern at low temperatures in the mixed valent compound NaV_2O_5.

1.3 CAD4, APEX, and HUBER diffractometers. Scanning procedures in SXD.

The laboratory SXD experiments were performed with an Enraf-Nonius CAD4 and a Bruker AXS APEX diffractometer, both using Mo-K_α radiation.

The CAD4 diffractometer consists of four circles, allowing the crystal

to be brought into various orientations. Two circles, denoted by Φ and χ, are used to adjust the crystal orientation relative to the diffractometer coordinate system. A third circle, ω, permits the orientation of the crystal lattice planes at a given angle ω to the direction of the primary beam, and finally, on the fourth circle, 2θ, the detector can be moved to be positioned at the angle 2θ to the primary beam. A schematic representation of the four circle geometry and the coordinate system used is given in Fig. 1.1. The primary beam direction, the crystal and the detector collimator are fixed in a horizontal plane. This plane is called the diffraction plane since every reciprocal lattice vector **h** has to be brought into this plane so that the Ewald diffraction condition can be realized. The plane of the χ circle is situated perpendicular to the diffraction plane. The Φ axis is the spindle axis of the goniometer head. The CAD4 diffractometer is equipped with a point detector, yielding a high angular resolution. This diffractometer has the disadvantage that a very large amount of time is necessary for collecting a full data set, due to the individual scanning of each reflection.

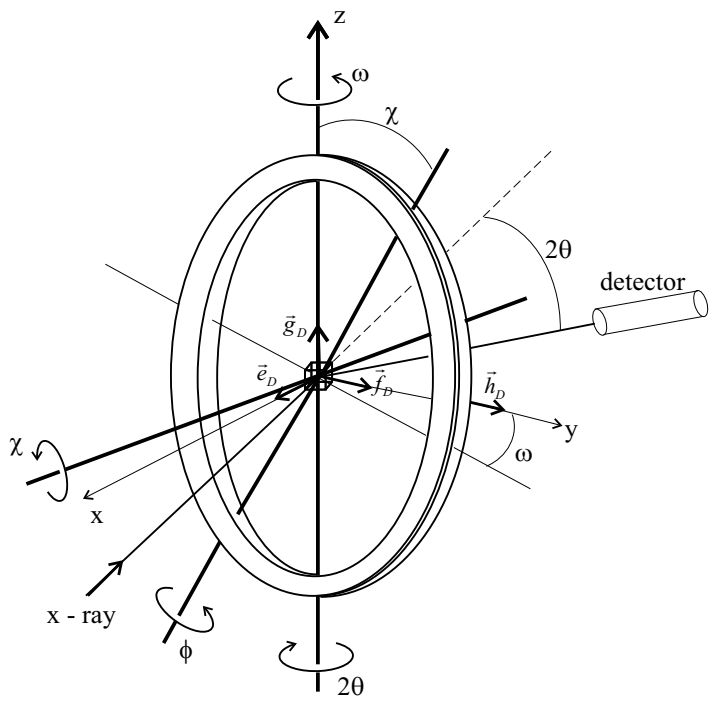

Figure 1.1: *Schematic representation of the four circles. The diffraction coordinate system with orthonormal unit vectors* $\mathbf{e_D}$, $\mathbf{f_D}$, $\mathbf{g_D}$ *is chosen such that* $\mathbf{g_D}$ *has the direction of the main axis, while* $\mathbf{e_D}$ *and* $\mathbf{f_D}$ *are in the diffraction plane.*

The APEX diffractometer has the χ angle fixed to 54.7° and is equipped with a two dimensional detector. The two-dimensionality of the detector covers a 2θ range of 60° for a fixed position of the detector at 6 cm distance

from the crystal. By varying ω, the reflections are brought in reflection conditions and their intensities are measured. By performing measurements at two different positions of the detector, a large 2θ range of 120° is covered. In a standard experiment, the crystal is exposed to the beam while ω changes within an interval of 180° with a step width of 0.3°. For each exposure a diffraction frame is recorded. Redundancy is obtained by collecting diffraction frames at three values of φ for the each 2θ and ω range. Thus, by measuring 3600 frames, we cover a large part of the Ewald sphere contributing to a very large data set collected in a reasonable amount of time (15 hours).

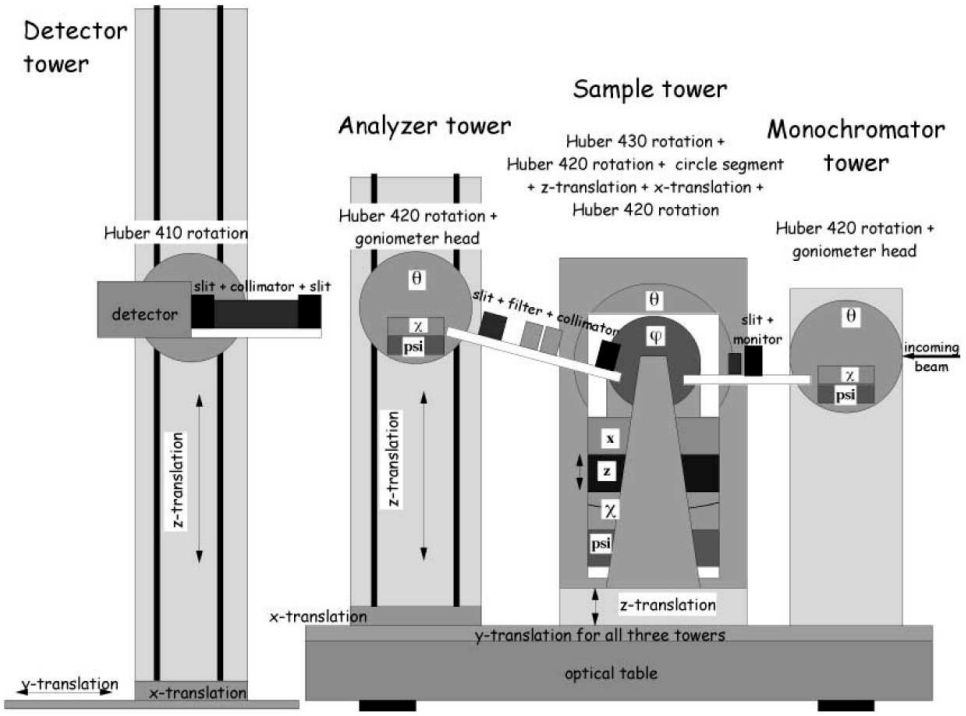

Figure 1.2: *Sketch of the HUBER diffractometer. The three towers are mounted together on an optical table. The detector is placed behind the diffractometer on a tower that can be translated in all three directions. The detector is kept parallel to the incoming beam by a rotation. Optical rails between the towers allow mounting of slit systems, colimators and beam monitors.*

The synchrotron SXD experiments were performed with a triple-axis HUBER diffractometer (Fig. 1.2), consisting of monochromator, sample and analyzer. The analyzer rotation determines the observed lattice spacing at the sample. We used a Si (3 1 1) crystal at 115 keV photon energy, which yield a 2θ angular resolution defined by the full width at half maximum FWHM of 0.0025°. Due to the low absorption at these high photon energies and small Bragg angles, the measurements were performed in transmission

geometry. Contrary to the above mentioned single crystal diffractometers (CAD4 and APEX), this instrument is operated with a vertical scattering plane. This diffractometer has four towers for monochromator, sample, analyzer and detector (Ge solid state). The monochromator and analyzer towers are equipped with a Huber 420 goniometer for the θ-rotation and a Huber 408 and a Huber 5202.5 circle segment for the crystal alignment. A circle segment with an angular range of $\pm$ 10° provides the χ-rotation. The low temperature measurements were performed using a displex cryostat. [3]

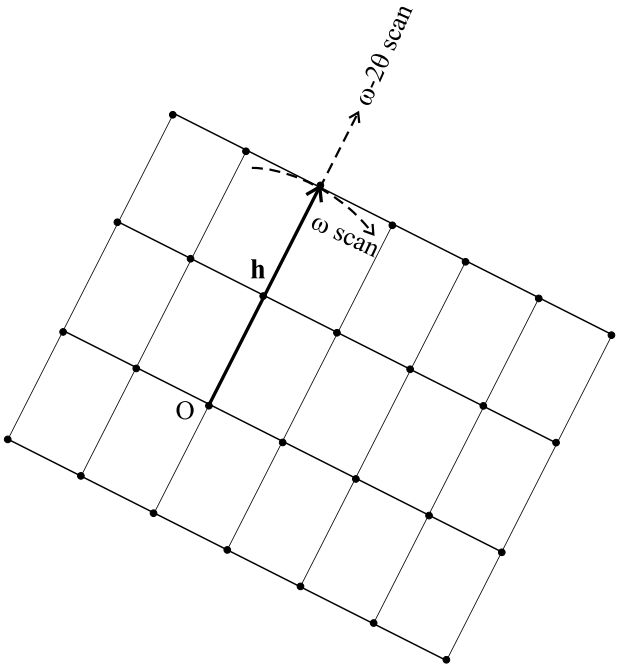

Figure 1.3: *Scan directions in the ω-scan and $\omega - 2\theta$-scan mode. The origin of the reciprocal lattice is denoted by O.*

Scanning procedures [4] in SXD can be used in two different ways: the "ω-scan" method and the "$\omega - 2\theta$-scan" method. In the ω-scan mode, the detector is held stationary at the theoretical 2θ angle of the actual reflection and the crystal and thus the corresponding reciprocal lattice vector $\mathbf{h}$ is rotated by an angular increment $\Delta\omega$. In the $\omega - 2\theta$-scan mode, both crystal and detector are moved. The crystal is rotated by $\Delta\omega$, while the detector is rotated in the 2θ circle with an angular velocity that is twice that of the crystal rotation, so that $\Delta 2\theta = 2\Delta\omega$. In terms of reciprocal lattice, in the ω-scan mode, the rotation takes place perpendicular to the reciprocal lattice vector $\mathbf{h}$, while in the $\omega - 2\theta$-scan mode, the scan is made in the direction of $\mathbf{h}$ (see Fig. 1.3). This statement applies only for the ideal situation where the incident beam is parallel, the source contain only one wavelength, the sample is point-shape with no mosaic spread and the detector has an infinitely

narrow aperture. In reality, the dimensions of the detector apertures which depend on the mosaic spread of the crystal as well as the spectral dispersion are critical for both type of scans [5].

With the CAD4 diffractometer, the two modes can be used in the individual scanning of each reflection. For the APEX diffractometer measurements, the two types of scans are performed simultaneously due to the two-dimensionality of the detector. Thus, the $\omega - 2\theta$-scans are resembled in the cross sections of the three-dimensional diffraction spots within a frame. The ω-scans are resembled in the rocking curves built by cross sections across the frames.

1.4 Space group determination

In this paragraph we describe the two main aspects for the space group determination in SXD analysis, *i.e.* the Laue symmetry and the systematic absences.

The symmetry properties of the unit cell can be transformed to the structure factor symmetry and further to the intensity symmetry. According to Friedel's law, for a reflection with the reciprocal lattice vector $\mathbf{h}$, $F(-\mathbf{h}) = F^*(\mathbf{h})$, resulting in the relation for the intensities of the reflections: $I(-\mathbf{h}) = I(\mathbf{h})$.

The symmetry elements of the real crystal lattice are directly related to the symmetry of the intensity distribution of the reciprocal lattice. These elements can be easily identified by comparing the intensities of the measured reflections. There are two rules for the space groups in the monoclinic system, as a representative example for all crystal systems:

1. A mirror plane† perpendicular to the y axis yields I(h k l) = I(h -k l). The same result is obtained for a mirror glide plane††, as the translational elements are added only to x and z. Thus, a mirror or glide plane in direct space causes a mirror in reciprocal space.

2. A two-fold axis††† in the b-direction yields I(k h l) = I(-h k -l). The same result is obtained when adding translational symmetry, resulting in screw axes††††. Thus, n-fold axes or screw axes in direct space cause n-fold axes in reciprocal space.

Taking into account the Friedel's law, additional conditions are obtained:

† The mirror plane is the symmetry element obtained by a reflection by a plane.

†† The glide plane is the symmetry element obtained by adding a displacement to a reflection, with the displacement vector having a direction parallel to the mirror plane.

††† The rotation axis is the symmetry element obtained by a rotation about an axis.

†††† The two-fold screw axis is the symmetry element obtained by adding a displacement to a rotation, with the displacement vector having a direction parallel to the rotation axis.

a) If I(h k l) = I(h -k l) then I(h k l) = I(-h k -l)

b) If I(h k l) = I(-h k -l) then I(h k l) = I(h -k l)

As for the monoclinic space groups, either a) or b) is valid, we obtain for the intensity symmetry:

I(h k l) = I(-h -k -l)= I(h -k l) = I(-h k -l)

This relation indicates that the intensity distribution is identical in four quadrants of reciprocal space.

Thus all the classes of a crystal system having the same intensity symmetry differing only by the inversion symmetry belong to the so called "Laue group". X-ray diffraction gives the symmetry of the intensity distribution, and not the crystal symmetry. Therefore a space group can not be uniquely identified because of the equivalence of the intensity symmetry for the space groups of the same Laue group.

However, in addition to symmetry in the intensity distribution, the translational parts of the symmetry elements will cause systematic absences for special groups of reflections. This property is of significant importance in space group determination. The following reflection conditions are established:

1) General reflection conditions: For a A, B, or C-centered lattice, only reflections (h k l) with k + l = 2n, h + l = 2n and h + k = 2n (n is an integer), respectively are present; For an F-centered lattice only reflections (h k l) satisfying simultaneously the conditions h + k, k + l, l + h = 2n are present; For an I centered lattice, only reflections (h k l) with h + k + l = 2n are present.

2) Zonal reflection conditions: If the glide plane is perpendicular to **a**, **b** or **c**-direction, the extinction affects reflections of type (0 k l), (h 0 l), or (h k 0) (*i.e.* for a glide plane perpendicular to the **b** direction, only reflections of type (h 0 l) with l = 2n are present).

3) Axial reflection conditions: If the screw axis coincides with **a**, **b**, or **c**, the extinction affects reflections of type (h 0 0), (0 k 0) or (0 0 l) (*i.e.* for a two-fold screw axis in the **b**-direction, only reflections of type (0 k 0) with k = 2n are present).

Some space groups can be uniquely determined from the recognition of the Laue symmetry or systematic absences. However, there are examples for which the space group determination from intensity symmetry and systematic absences is not unique. One of the problems is the decision whether a crystal belongs to a non-centrosymmetric or the corresponding centrosymmetric space group, since the Laue symmetry always indicates the corresponding centrosymmetric class (Friedel's law). In some of these cases, the physical properties of the compound are useful for space group determination. Moreover, when dispersion corrections are taken into account, Friedel's law is still valid for centrosymmetric structures but not in the noncentrosymmetric case. Thus, the effect of the dispersion corrections

can be used to distinguish between the centrosymmetric and the noncentrosymmetric space groups.

Difficulties in space group determination can be caused by twinning which will strongly affect the measured intensities. In the next paragraph we will introduce the concept of twinning and we will discuss the twin detection methods and the twin model determination for a precise SXD refinement.

1.5 Twin detection using the ω-scan

The twinned microstructures are a result of a polymorphic transformation when a higher symmetry crystal is cooled and converts to a lower symmetry structure. It is well known that the perovskites are susceptible to the formation of twins due to transitions between different phases during crystal growth process. The structural differences between one phase and another are very small. This makes a precise structure determination very difficult. Twinned microstructures can be described, by using the ferroelasticity concept. A ferroelastic phase results from the transformation of a paraelastic phase which is crystallographically more symmetrical. A ferroic crystal has in the absence of an external field (a mechanical strain field, electric field or magnetic field), two or more orientation states with well defined relationships. Symmetry breaking at the phase transition gives rise to such energetically equivalent domain states related to each other by the lost symmetry elements of the paraelectric phase. The domains are separated by mobile interfaces which can move under the effect of a temporary external mechanical stress. It was shown by Aizu [6] that the maximum number of orientation states that may be observed equals the number of symmetry operations lost by the crystal during the phase transformation. This number is calculated by n = order(G_P)/order(G_F), where G_P and G_F are the point groups of the paraelastic and ferroic phase respectively.

The twins can be classified into two species [7]:

a) The merohedral twins showing a single orientation of the reciprocal lattice and thus giving rise to single diffraction spots. They are optically indistinguishable and their presence may be indicated by a high R-value caused by large differences between the observed and calculated intensities in the crystal structure determination. A careful analysis of the intensity distribution is necessary for the twin model determination.

b) The pseudo-merohedral twins characterized by two or more reciprocal lattices differently oriented are giving rise to double or multiple spots. Such twinning can be detected due to the slight deviation in ω of the reciprocal lattices which gives rise to splitting of the reflections. This deviation can be easily recognized in the splitting of the reflections caused by the double

or multiple spots. The spots around one reciprocal lattice point appear at almost the same 2θ but at different values of ω. Thus the splitting of the reflections caused by this type of twinning can be detected in the ω-scans. The intensity distribution around a reciprocal lattice point caused by pseudo-merohedral twinning can be mapped by performing different ω-scans in the direction perpendicular to the reflection plane (the plane of the χ circle). Such ω-scans performed for different values of χ will be referred in this thesis as ω - χ scans.

In Fig. 1.4 we illustrate an example of a pseudo-merohedral twinning as a result of a transition from an orthorhombic to a monoclinic symmetry. The projection along the **b** axis of a monoclinic lattice with $\beta \cong 90°$ is shown, together with its twin lattice. The monoclinic twin lattices are symmetrically distributed with respect to the averaged orthorhombic lattice. The twin operation is the mirror plane perpendicular to **a**. The ω misfit is intentionally exaggerated. By measuring the reflections in the direction perpendicular to the lattice vectors (ω-scans), the splitting of the reflections due to twinning can be determined.

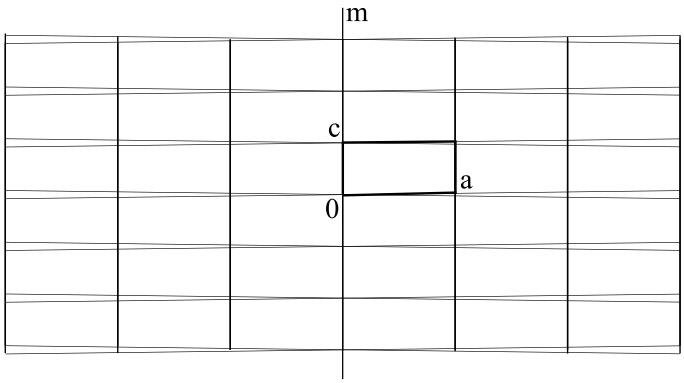

Figure 1.4: *Example of a pseudo-merohedral twin resulted from a transition from orthorhombic to monoclinic symmetry.*

The detection of the splitting of the reflections due to twinning, which is usually very small, necessitates high angular resolution measurements. Therefore, it is advantageous that the ω-scans are performed using the CAD4 diffractometer equipped with a point detector.

However, once the twinning is detected and thus the correct space group is assigned, we will perform structural refinements on full data sets collected with the APEX diffractometer. The intensities of the reflections are measured in a standard experiment and by means of refinement, the positions of the atoms in the unit cell are determined. The poor angular resolution of the APEX diffractometer does not always allow us the separation of the twin fractions resulting in averaged lattice parameters (to their values

in the higher symmetry structure). The observed intensities of the reflections in the case of a twinned crystal, are the sums of the intensities of the contributing twins fractions to the respective reflections. A detwinning process is therefore necessary to find the intensities corresponding to one twin fraction, such that precise positions of the atoms in the unit cell can be determined.

1.6 Bond valence sum method

In standard SXD analysis, the calculation of the bond lengths from the refined positions of the atoms allows the determination of the valence of the atoms by using the bond valence sum method. This method serves to determine the valences of atoms in a chemical compound by the sum of the bond valences for all bonds, in which the atoms participate. Thus for a mixed valent compound, the valence $V(i)$ of an atom i in the crystal structure is calculated as the sum of contributions of the bonds of atom i towards the atoms j in its first coordination shell:

$V_i = \sum v_{ij}$

$v_{ij} = exp[(R_{ij} - d_{ij})/b]$,

where v_{ij} is the bond valence of the atom pair (i, j), $b = 0.37$ Å is an universal parameter and R_{ij} is an empirical parameter determined for almost any pair of atoms from fitting the atomic valences for many different compounds at room temperature [8, 9].

Taking the example of NaV_2O_5, for the vanadium-oxygen pair R_{ij} depends on the valence state of vanadium. The reported values for the two valence states of vanadium, V^{4+} and V^{5+} are: $R^{4+} = R(V^{4+}\text{-}O) = 1.784$ Å and $R^{5+} = R(V^{5+}\text{-}O) = 1.803$ Å, respectively [8].

The accuracy of the BVS method relies on the precise determination of the values of the bond lengths derived from refinements of the atoms positions in the correct space group. However, as we will extensively discuss throughout the Chapter 2, the space group determination for the low temperature phase of NaV_2O_5 is very difficult.

1.7 Resonance x-ray scattering

The scattering amplitude of the atom can be written in a general form: $f(\mathbf{Q}, \omega) = f^0(\mathbf{Q}) + f'(\omega) + if''(\omega)$. The Thomson term, $f^0(\mathbf{Q})$, represents the Fourier transform of the atomic charge distribution and depends only on the scattering vector $\mathbf{Q}$. The resonant scattering terms, $f'(\omega)$ and $f''(\omega)$, are the real and imaginary parts of the dispersion corrections and depend only on the photon energy. The imaginary part is proportional to the absorption cross section. Thus, by measuring the absorption cross section, it is possible

to determine $f''(E)$ and by using Kramers-Krönig transformation, $f'(E)$ can be obtained. The effect of the resonant scattering terms $f'(E)$ and $f''(E)$ becomes significant when the x-ray energy is close to one of the absorption edge energies of an atom of the target material. [10]

The resonance x-ray scattering technique can be used to generate contrast for one particular element by using a fixed photon energy or to generate large intensity modulations by scanning the photon energy of particular Bragg reflections. As we will present in the Chapter 2, the resonance x-ray scattering has been used in the determination of the charge order pattern in NaV_2O_5. By using resonance x-ray diffraction experiments near the vanadium K-absorption edge ($E_A \approx 5.456$ keV) the small difference of atomic scattering factors between V^{4+} and V^{5+} is enhanced with a large modulation [11]. The difference between the V^{4+} and V^{5+} is obtained from the scattering intensity of particular reflections as a function of energy across E_A. By using the different charge order pattern models, the scattering intensity of these reflections are calculated and are compared to the measured ones.

References

[1] M. A. Korotin, I. S. Elfimov, V. I. Anisimov, M. Troyer, D. I. Khomskii, Phys. Rev. Lett. **83**, 1387 (1999).

[2] Y. Ueda, Chem. Matter. **10**, 2653 (1998).

[3] U. Rütt, M. A. Beno, J. Strempfer, G. Jennings, C. Kurtz, and P. A. Montano, Nuclear Instr. and Methods in Phys. Research A **467-468**, 1026 (2001).

[4] P. Luger, *Modern X-ray Analysis on Single Crystals* (Walter de Gruyter, Berlin, New York, 1980).

[5] R. D. Burbank, Acta Cryst. **17**, 434 (1964).

[6] K. Aizu, Phys. Rev. B **2**, 754 (1969).

[7] C. Giacovazzo, H. L. Monaco, D. Viterbo, F. Scordari, G. Gilli, G. Zanotti, and M. Catti, *Fundamentals of Crystallography* (Oxford University Press, New York, 1992).

[8] N. Brese and M. O'Keeffe, Acta Crystallogr. B **47**, 192 (1991).

[9] M. O'Keeffe and N. Brese, Acta Crystallogr. B **48**, 152 (1992).

[10] J. Als-Nielsen and D. McMorrow, *Elements of Modern X-Ray Physics* (John Wiley & Sons, Ltd, 2001).

[11] H. Nakao, K. Ohwada, N. Takesue, Y. Fujii, M. Isobe, Y. Ueda, M. v. Zimmermann, J. P. Hill, D. Gibbs, J. C. Woicik, i. Koyama, and Y. Murakami, Phys. Rev. Lett. **85**, 4349 (2000).